
Solution and Solid-State Studies of Alkali Metal Aggregate Assemblies

John Jacob Morris

Publication Date

07-04-2008

License

This work is made available under a All Rights Reserved license and should only be used in accordance with that license.

Citation for this work (American Psychological Association 7th edition)

Morris, J. J. (2008). *Solution and Solid-State Studies of Alkali Metal Aggregate Assemblies* (Version 1). University of Notre Dame. <https://doi.org/10.7274/br86b27956f>

This work was downloaded from CurateND, the University of Notre Dame's institutional repository.

For more information about this work, to report or an issue, or to preserve and share your original work, please contact the CurateND team for assistance at curate@nd.edu.

CHAPTER 2

MANIPULATION OF MOLECULAR AGGREGATION AND EXTENDED SUPRAMOLECULAR STRUCTURE USING SELF-ASSEMBLED LITHIATED MIXED-ANION COMPLEXES

2.1 Introduction

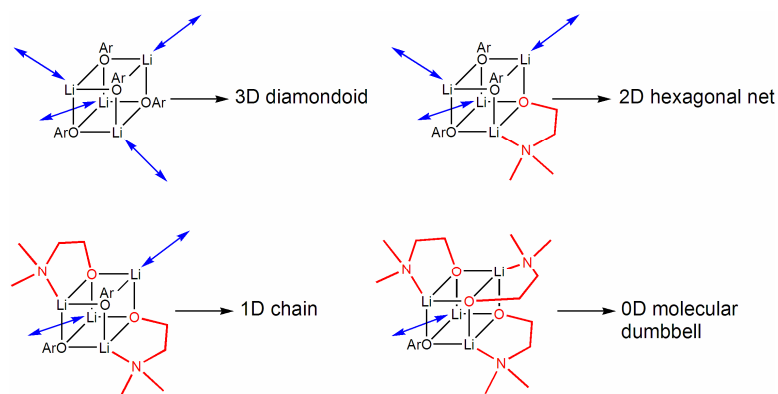
The synthesis and characterization of extended coordination network assemblies continues to be an area of intense interest due to the potential of periodic materials in numerous applications.¹ A common strategy for the synthesis of networks is the building-block approach, in which isolated metal centers or metal clusters are linked by bridging organic ligands.² The choice of metal center often dictates the architecture of the resultant framework owing to a distinct preference for a certain geometry and coordination number. However, the rational design of specific network structures *a priori* remains problematic.³ Researchers have used a number of creative methods to help control the structure and dimensionality of extended materials.⁴ A common approach is to make systematic modifications to the reactions including: altering the length of the bridging ligand;⁵ changing the metal;⁶ switching solvents, anions, or guest molecular templates present in the final network structure;⁷ varying the denticity of the linker molecule;⁸ and adjusting the reaction conditions such as the temperature⁹ or pH.¹⁰

A powerful emerging paradigm in network synthesis is that a relatively small number of high-symmetry topologies dominate the structures of extended frameworks.¹¹ For example, diamondoid and primitive cubic nets are by far the most common 3D arrangements arising from the combination of tetrahedral and octahedral nodes bridged by linear linkers. In addition, the structures of many 1D and 2D polymers can be considered as components of these high-symmetry 3D networks. However, only a few studies have been devoted to experimentally establishing the nature of the relationship between closely related 1D, 2D and 3D nets.¹²

Work in our group has focused on the use of structurally well-defined s-block metal aggregates as secondary building units (SBUs).¹³⁻¹⁵ This approach compensates for the lack of directionality commonly associated with alkali metal ions. Our initial work, which was highlighted in the introductory chapter, investigated the use of Li_4O_4 tetrameric cubanes formed by lithium aryloxides as SBUs.^{13a} These complexes are excellent candidates as building blocks since they are readily pre-assembled in solution, contain strong Li-O bonding, and the metals are held in a tetrahedral arrangement with one coordination site available for possible polymer extension. We have demonstrated that these aggregates can be used to build 3D diamondoid, and related lower dimensionality polymers, through the use of neutral linking molecules.^{13a} Similarly, we have used sodium aryloxides to construct primitive cubic networks from hexameric Na_6O_6 SBUs.^{13b,13f}

We wished to add another level of sophistication to these systems by controlling the number of metal atoms within each aggregate that may act as points of network extension. During our studies we discovered that crystallization of lithium 2,4,6-

trimethylphenoxide (ArOLi) from dioxane solution leads to formation of a diamondoid network constructed from tetrameric aggregates. This was chosen as an archetypal system for modification. Lithium dimethylaminoethoxide (ROLi) was selected as the second component of the proposed mixed-anion system,¹⁶ as the formation of five membered O-C-N-Li chelate rings appeared feasible.¹⁷ As shown in Scheme 2.1, our initial aim was to systematically vary the stoichiometry of the two anionic components within a tetrameric Li_4O_4 cubane aggregate, and in turn control the dimensionality of the resulting polymer. Our expectation was that a stepwise reduction in dimensionality starting from a 3D diamondoid network would result in a 2D hexagonal net, a 1D zig-zag chain, and finally a 0D dumbbell arrangement. This strategy has proved largely successful, with one unexpected caveat. Specifically, altering the stoichiometry of the anions not only changed the dimensionality of the polymer, but also switched the basic molecular aggregation from tetrametallic to hexametallic.

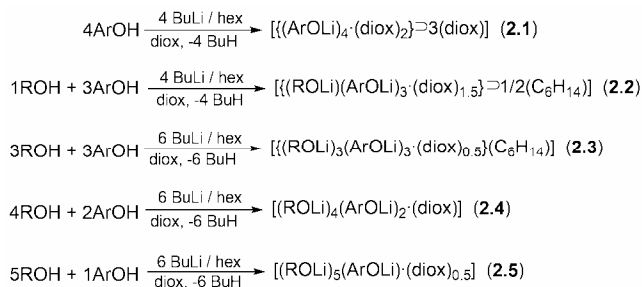


Scheme 2.1 Proposed sequential replacement of aryloxide anions (ArO) by chelating dimethylaminoethoxide units, and the effect on the resulting supramolecular structure. The blue arrows represent the sites for polymer extension.

2.2 Results and Discussion

2.2.1 Synthesis

All complexes were prepared by dissolution of the alcohol(s) in 1,4-dioxane, followed by deprotonation with ⁿBuLi at ambient temperature. The stoichiometric ratios used for each of the reactions and the resulting products crystallized are detailed in Scheme 2.2. The reaction involving only 2,4,6-trimethylphenol produced crystalline material **2.1** on storage of the solution under ambient conditions for two days. The remaining reactions all produced an instant precipitate on addition of ⁿBuLi. High quality crystals of **2.2-2.5** were prepared by dissolving each precipitate in a solution of dioxane and hexane, followed by slow cooling to ambient temperature.



Scheme 2.2 Preparation of **2.1-2.5**

Compounds **2.1-2.5** were all characterized by ¹H and ¹³C NMR spectroscopy, and also by single-crystal X-ray diffraction. The following discussion will detail the basic molecular cage aggregates present, followed by an analysis of their metrical data, and conclude with a summary of the extended supramolecular architectures produced. After the discussion of the five targeted compounds there will be a brief analysis of $[(\text{ArOLi}) \cdot (\text{ROH}) \cdot (\text{diox})_{0.5}]$ (**2.6**), which was synthesized inadvertently during the targeted synthesis of **2.3** due to insufficient base present.

2.2.2 Molecular Structures

The molecular component of $[\{(ArOLi)_4 \cdot (diox)_2\} \supset 3(diox)]_{\infty}$ (**2.1**) is a tetrameric cubane aggregate (Figure 2.1). Tetrameric aggregation was anticipated, since our previous work with lithium aryloxide/dioxane systems has shown that cubanes dominate unless there is significant steric hindrance at the *ortho*-positions of the phenyl ring or alternatively if the aromatic ring is substituted by a strongly electron-withdrawing group.^{13,18,19} Each of the four lithium centers in **2.1** are solvated by a dioxane and all of the dioxanes bridge to neighboring aggregates.

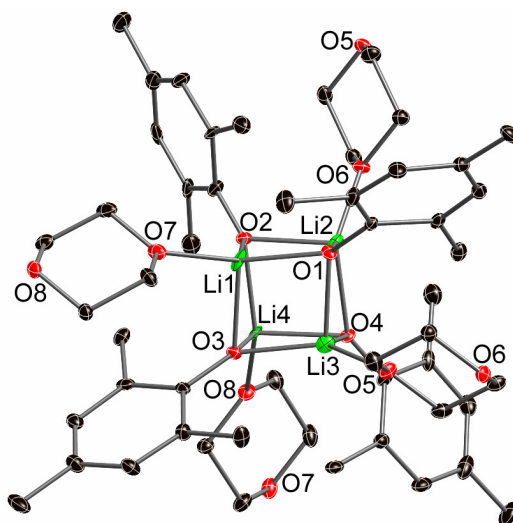


Figure 2.1 Tetrameric cubane SBU in **2.1**, showing all four lithium centers connected to dioxane. Hydrogen atoms removed for clarity.

The first attempt to form a mixed-anion compound involved a 3:1 ratio of ArOLi:ROLi. This reaction successfully led to the formation of $[\{(ROLi)(ArOLi)_3 \cdot (diox)_{1.5}\} \supset 1/2(C_6H_{14})]_{\infty}$ (**2.2**), which contains the appropriate ratio of anionic components. As shown in Figure 2.2, the molecular building block is the desired mixed-anion cubane, composed of three ArOLi and one ROLi units. Three of the lithium

atoms are solvated by dioxane molecules, with the fourth lithium chelated by the nitrogen of the alkoxide ligand. Again, all three dioxanes bridge to neighboring cubanes.

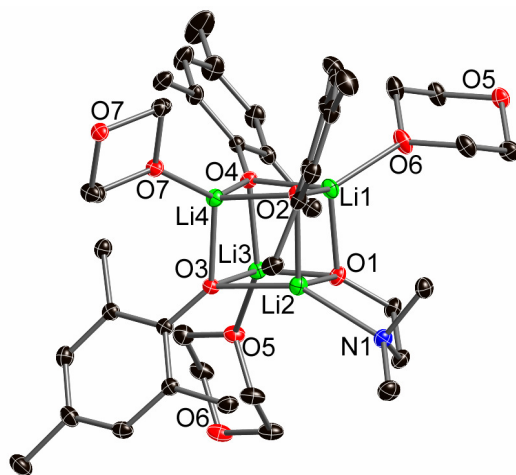


Figure 2.2 Mixed-anion (3:1) tetrametallic SBU in **2.2**, showing one chelated and three dioxane-solvated lithium centers. Hydrogen atoms removed for clarity.

The next compound targeted was a tetrametallic aggregate with a 2:2 ratio of ArOLi to ROLi. To our initial surprise, the compound prepared was $[(\text{ROLi})_3(\text{ArOLi})_3 \cdot (\text{diox})_{0.5}](\text{C}_6\text{H}_{14})_\infty$ (**2.3**). This complex does contain equivalent amounts of the two anions as anticipated, but is a hexametallic 3:3 complex with a Li_6O_6 prismatic core (Figure 2.3). The formation of the larger aggregate is rationalized by the reduction in steric hindrance upon incorporation of more than one ROLi unit in the mixed-anion complex. This view is supported on considering the structure of $[\text{Me}_2\text{N}(\text{CH}_2)_2\text{OLi}]_8$ (**2.7**), which forms an octameric aggregate where all of the lithium atoms are chelated by a dimethylamido nitrogen unit (Figure 2.4).¹⁷ In **2.3**, the combination of the three aryloxy and three alkoxide groups within a single complex leads to stabilization of the intermediate hexametallic aggregate.

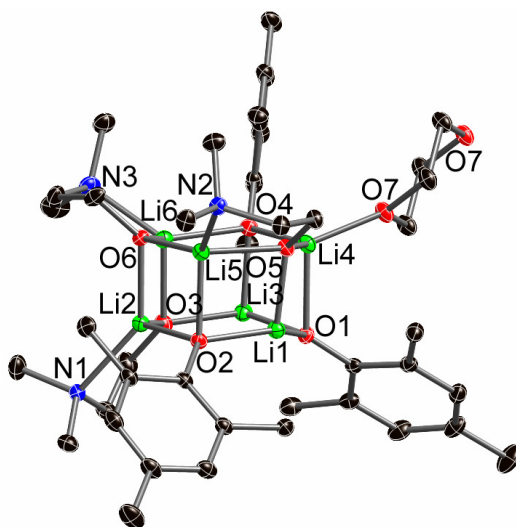


Figure 2.3 Mixed-anion (3:3) hexametallic SBU in **2.3**, showing three chelated, one dioxane-solvated and two unsolvated lithium centers. Hydrogen atoms removed for clarity.

Another unexpected feature of **2.3** is that only four of the six metals are solvated by Lewis base, three by chelation of the dimethylamido units and one by a bridging dioxane. The two remaining lithiums are only three coordinate. This is likely due to the limited space available for solvation of these centers in the 3ArOLi:3ROLi aggregate. Indeed, each three coordinate metal center has one short Li-C contact of ~ 2.6 Å to a methyl group on an aromatic ring, whereas the remaining contacts are ≥ 3.0 Å.

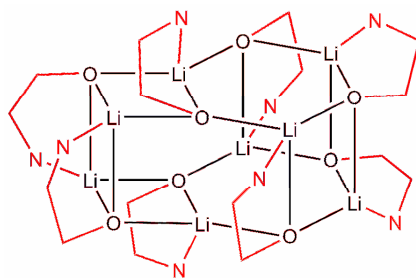


Figure 2.4 Octameric structure of $[\text{Me}_2\text{N}(\text{CH}_2)_2\text{OLi}]_8$, **2.7**, with chelate rings highlighted in red and the methyl groups on nitrogen removed for clarity.¹⁷

Upon the realization that hexametallc aggregation was viable, the formation of a 2:4 complex of ArOLi to ROLi was investigated. This proved possible, and the complex $[(\text{ROLi})_4(\text{ArOLi})_2\cdot(\text{diox})]_\infty$ (**2.4**) was subsequently synthesized and characterized. As shown in Figure 2.5, a Li_6O_6 cage is again produced, this time with two aryloxy and four alkoxide anions. As expected, four of the metals are chelated while the two others are coordinated by dioxane molecules. Both dioxanes also bridge to neighboring aggregates.

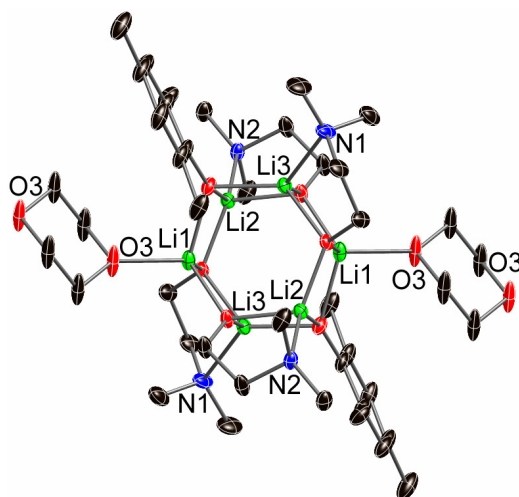


Figure 2.5 Mixed-anion (2:4) hexametallc SBU of **2.4**, showing four chelated and two dioxane-solvated lithium centers. Hydrogen atoms removed for clarity.

The final compound targeted to complete the stoichiometric series was the hexametallc aggregate with a 1:5 ratio of ArOLi to ROLi present. As shown in Figure 2.6, the complex $[(\text{ROLi})_5(\text{ArOLi})\cdot(\text{diox})_{0.5}]_\infty$ (**2.5**) was prepared and contains the correct ratio of anions within a hexametallc aggregate. Five of the metal centers are chelated by dimethylamido groups, and the remaining single metal is coordinated to a dioxane molecule, which bridges between two aggregates.

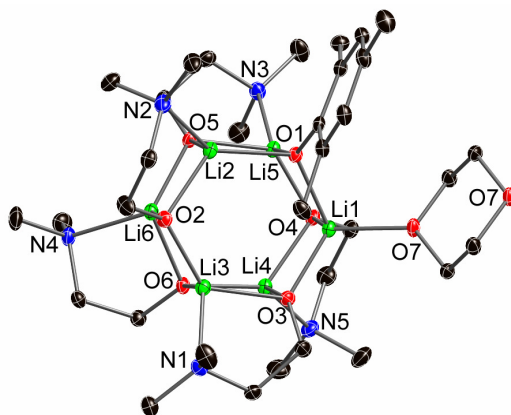


Figure 2.6 Mixed-anion (1:5) hexametallic SBU of **2.5**, showing five chelated and one dioxane-solvated lithium centers. Hydrogen atoms removed for clarity.

A feature of interest in **2.3-2.5** is the positions adopted by the chelate rings. The possibility of chelation to various metal centers within an aggregate, termed chelate isomerization, has been studied previously for alkali metal complexes.^{20,21} In general, five-membered ring chelation occurs along the Li_3O_3 faces in homoleptic, prismatic hexamers to give structures with approximate S_6 symmetry, *i.e.* alternating ‘top’ and ‘bottom’ chelation (Figure 2.7).²¹ This coordination mode is consistent with the structures of **2.4** and **2.5**. However, complex **2.3** has two of its three chelate rings on a single Li_2O_2 face, as would be found in a D_3 symmetric structure. This anomalous arrangement is probably a consequence of the unsymmetrical nature of the mixed-anion complex.

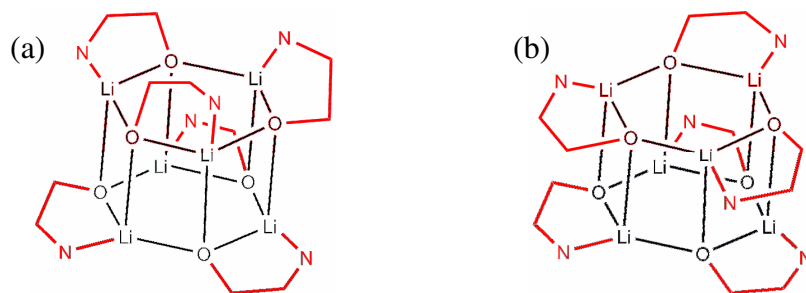


Figure 2.7 Possible chelation modes of homoleptic lithium aminoethoxide aggregates with resulting (a) S_6 and (b) D_3 symmetry.

Table 2.1 lists selected bond lengths and angles for **2.1-2.5** and **2.7**. The Li-O_{diox} distances lie in a relatively tight range, between 1.935(2)-2.049(5) Å. These values are consistent with normal solvation, indicating that bridging of dioxane between two aggregates does not significantly perturb the dative bonding.²² The Li-N distances for **2.2-2.5** and **2.7** are also in accord with expectations, ranging between 2.081(4)-2.286(4) Å. Similar, relatively wide ranges are found for previously published structures containing five-membered Li-O-C-C-N(Me₂) rings (mean 2.15 Å).²² A general pattern is that the longer Li-N distances are correlated with more acute chelate N-Li-O_R bite angles. For example, in **2.4** the Li-N distances of 2.081(4) and 2.286(4) Å are correlated with N-Li-O_R bite angles of 89.68(16) and 86.15(15)° respectively.

A final characteristic of note is that the mean Li-O_{Ar} distances are consistently longer than mean Li-O_R distances. The mean Li-O_{Ar} distances range between 1.964(6)-1.997(3)°, whereas the mean Li-O_R distances range between 1.897(4)-1.937(2)°. This noticeable difference in bond lengths is associated with both the relative size of the anions and also variations in their electronic nature. Similar effects have been noted previously for lithiated mixed aryloxide/alkoxide aggregates.²³ The significance here is that the related enthalpic stabilization accompanying incorporation of alkoxide units in the aryloxide aggregates helps rationalize the ability to prepare the unusually large set of stoichiometric variants, *i.e.* 3:1, 3:3, 2:4, and 1:5.

TABLE 2.1

KEY BOND LENGTHS [\AA] AND ANGLES ($^\circ$) FOR **2.1-2.5** and **2.7**. MEAN PARAMATERS ARE SHOWN IN BRACKETS

Compound	Aggregate	Extended Structure	Li-O _{Ar}	Li-O _R	Li-O _{diox}	Li-N	Chelate N-Li-O _R
2.1	Tetramer	3D Diamondoid	1.959(5)-2.045(5) <1.997(5)>	—	1.937(5)-2.049(5) <1.992(5)>	—	—
2.2	Tetramer	2D Hexagonal	1.982(3)-2.010(3) <1.981(3)>	1.857(3)-1.920(3) <1.897(3)>	1.957(3)-1.996(3) <1.978(3)>	2.211(4)	84.04(13)
2.3	Hexamer	0D Dumbbell	1.920(3)-2.071(2) <1.964(6)>	1.834(2)-1.949(2) <1.906(2)>	1.935(2)	2.103(2)-2.165(2) <2.124(2)>	87.83(9)-90.39(9) <89.15(9)>
2.4	Hexamer	1D Chain	1.948(5)-2.062(4) <1.991(6)>	1.880(4)-1.915(4) <1.925(4)>	1.992(4)	2.081(4),2.286(4) <2.183(4)>	86.15(15), 89.68(16) <87.92(16)>
2.5	Hexamer	0D Dumbbell	1.950(3)-2.022(2) <1.975(2)>	1.874(2)-1.969(2) <1.920(3)>	1.994(2)	2.096(3)-2.196(3) <2.124(3)>	84.37(9)-90.05(10) <88.38(10)>
2.7	Octamer	—	—	1.894(2)-1.994(2) <1.937(2)>	—	2.114(2)-2.189(2) <2.150(2)>	87.15(9)-90.25(10) <88.67(9)>

2.2.3 Extended Supramolecular Structures

All four lithiums in the tetrameric cubanes of **2.1** are coordinated by dioxane molecules that bridge to neighboring aggregates. The Li_4O_4 units act as tetrahedral nodes to give a 3D cubic diamondoid network (Figure 2.8). The network is quite open, with large I-shaped channels of $3.0 \times 9.7 \text{ \AA}$ running parallel to both the *a*- and *b*-axes of the crystal.²⁴ The channels are filled with approximately three disordered dioxanes per Li_4O_4 tetrameric unit (as modeled using the SQUEEZE routine of PLATON).²⁵ Calculations indicate that 34.6% of the total volume within the crystal would be solvent accessible space upon removal of the free dioxane guest molecules.²⁵ As a comparison, our recently reported 3D diamondoid structure of $[(1\text{-naphthOLi})_4(\text{diox})_2]_\infty$, contains rectangular channels of $5.0 \times 9.5 \text{ \AA}$, with a potential solvent accessible volume of 34.8%.^{13a}

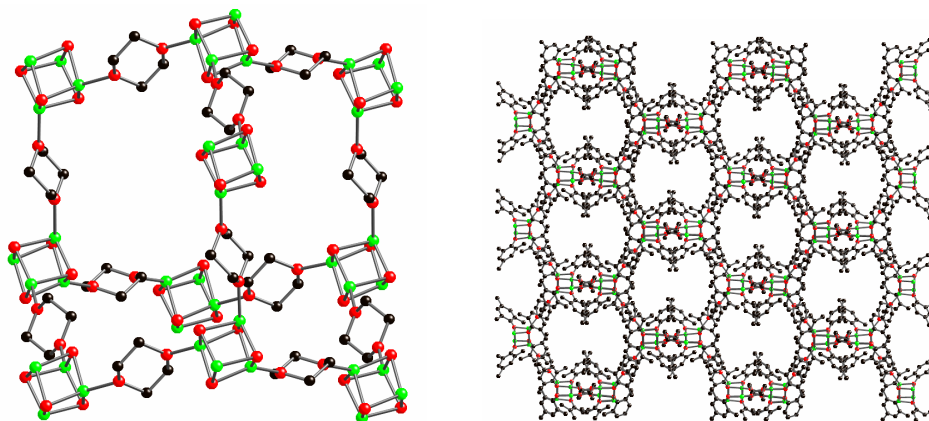


Figure 2.8 Views of a single adamantane subunit of **2.1**, and the extended 3D diamondoid network highlighting the I-shaped open channels (enclathrated dioxane molecules are removed for clarity).

Assembly of the tetrametallic $3\text{ArOLi}:1\text{ROLi}$ aggregate **2.2** resulted in blocking a single metal site through chelation, as originally intended. The remaining three lithium centers coordinate to bridging dioxane molecules, in turn leading to formation of a 2D

hexagonal, 6^3 -network (Figure 2.9).²⁶ In the crystal, the 2D sheets are aligned so that channels of 3.2×7.4 Å are created parallel to the *c*-axis.²⁴ These channels are filled with disordered solvent molecules, most likely hexane based on the ^1H NMR data of the crystals.

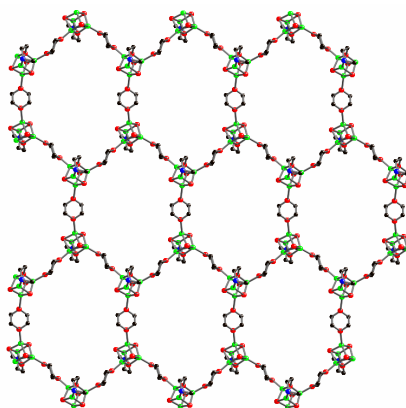


Figure 2.9 Extended 2D 6^3 -net of **2.2** showing only the Li_4O_4 cubanes and the other framework atoms.

It is informative to analyze the gross structural variations between the closely related 3D and 2D frameworks **2.1** and **2.2**. The centroid-centroid separations of neighboring cubanes are similar in **2.1**, at 9.73 Å (the centroid is defined as the center of the Li_4 tetrahedron). In comparison, these distances vary more widely in **2.2**, with two longer edges of the distorted hexagonal rings at 9.73 Å, and four shorter edges at 9.63 Å. The longer edges have correspondingly longer $\text{Li}-\text{O}_{\text{diox}}$ distances of 1.996(3) Å, compared with 1.982(3) and 1.957(3) Å for the shorter edges. Also, the bridging dioxane molecules can pivot within the $\text{Li}-\text{Li}$ vector defined between linking cubanes, thus changing the distance between neighboring aggregates.

Another series of revealing measurements are the angles made between connecting centroids. In **2.1** there are three independent angles, 103.30, 111.21 and

114.06°, whereas there are only two angles of 103.04 and 125.01° in **2.2**. These distortions from the ideal tetrahedral node angle of 109.5° permits tuning of the cavity volume to most effectively fill space within the diamondoid and hexameric scaffolds.²⁷ In addition, this flexibility is likely important for effective packing in the crystal.

The next extended structure targeted was a 1D zig-zag chain polymer composed of 2ArOLi:2ROLi linked tetramers. As noted above, the equimolar reaction of ArOLi and ROLi produced the 0D dumbbell structure **2.3** (see later). However, once the hexametallic core was identified as a possible SBU we next focused on a 2ArOLi:4ROLi stoichiometry. Subsequently, complex **2.4** was prepared and found to form a 1D chain. The hexametallic core contains four chelated lithium centers, with the two remaining metals connected to dioxane molecules that bridge to other aggregates. As seen in Figure 2.10, the chain is linear, with the dioxane molecules binding to the opposites ends of the Li₆O₆ cores. The only other hexametallic lithium aggregate known to form a coordination polymer is the morpholine adduct [Li₆Cl₆(HMorph)₃]_∞.²⁸ In that case all of the morpholine molecules bridge to create a 3D primitive cubic network.

The final remaining extended structure to be rationally constructed in this series was a 0D dumbbell using a 1:5 ratio of ArOLi to ROLi. As shown in Figure 2.11, complex **2.5** meets these expectations. Two hexametallic aggregates are joined through a single bridging dioxane, with the five remaining lithium centers chelated by dimethylamido units. Although dumbbells are unusual, a number of these structures have been reported utilizing alkali metal aggregates,²⁹ including ones formed with dioxane.³⁰ The dumbbell motif is interesting as it can be considered to be an intermediate between a completely solvated 0D molecular compound and an extended supramolecular polymer.

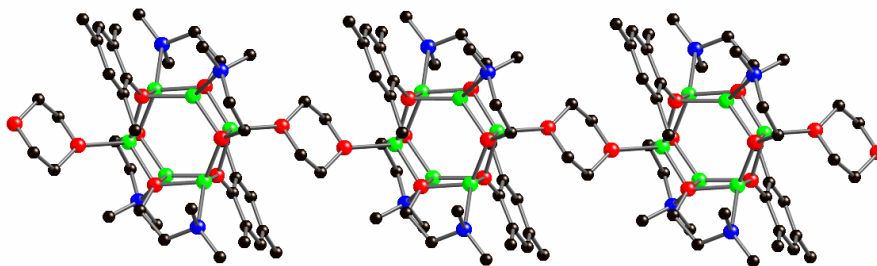


Figure 2.10 Section of the 1D linear chain polymer of **2.4** composed of linked hexametallic aggregates.

The one complex in the series **2.1-2.5** that does not fit the extended structure pattern is the 3:3 mixed anion **2.3**. Since three of the lithium centers in the aggregate are chelated, there are three remaining metals available for network extension. The expectation is that a 2D hexagonal network (related to **2.2**) would result. However, only one of the lithium centers is coordinated by dioxane, forming the 0D dumbbell structure shown in Figure 2.12. The remaining two lithium centers are three coordinate. As previously discussed this is likely a consequence of steric encumbrance at these metal sites within the hexametallic core. Overall, the dumbbell structure of **2.3** is similar to that of **2.5**, with the distance between the two centroids of the Li_6O_6 units in **2.3** and **2.5** being 10.7 and 10.6 Å, respectively.

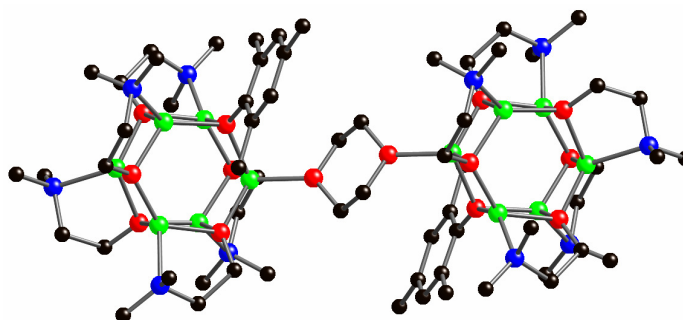


Figure 2.11 The 0D molecular dumbbell structures of **2.5**. Hydrogen atoms are removed for clarity.

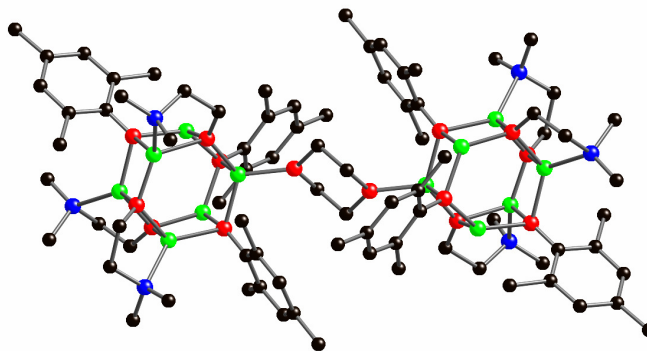


Figure 2.12 The 0D molecular dumbbell structure of **2.3**. Hydrogen atoms are removed for clarity.

2.2.4 Synthesis of a dimethylethanolamine solvate

During the initial synthesis of **2.3**, an insufficient amount of lithium base was used to deprotonate the 3:3 ratio of 2,4,6-trimethylphenol to dimethylethanolamine resulting in the formation of $[(\text{ArOLi})\cdot(\text{ROH})\cdot(\text{diox})_{0.5}]$ (**2.6**). Complex **2.6** is composed of two lithium 2,4,6-trimethylphenoxide monomers that are chelated by non-deprotonated dimethylethanolamine, and bridged by a molecule of dioxane, as shown in Figure 2.13. Further aggregation through dioxane solvation is inhibited as each metal is tetracoordinate and hence coordinatively saturated.

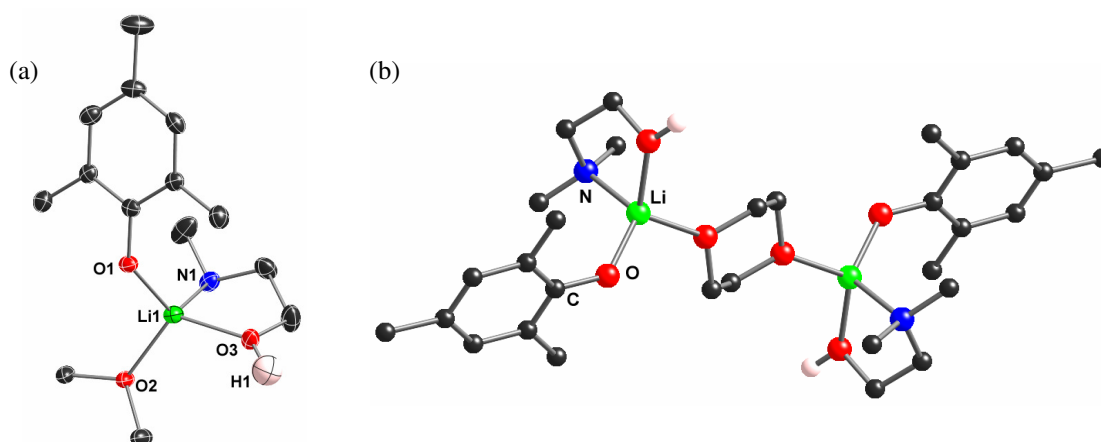


Figure 2.13 (a) The asymmetric unit of monomeric **2.6**. (b) The supramolecular dimer of **2.6** formed by the bridging dioxane molecule. Only the proton found in the electron difference map is shown for clarity.

For the previous set of compounds, **2.1-2.5**, the Li-O_R distance was moderately shorter than the Li-O_{Ar} distance in the aggregates as highlighted in Table 2.1. Since the oxygen of dimethylethanolamine in **2.6** coordinates to the lithium as a Lewis base instead of an anion, the Li-O_R distance of 1.953(5) Å is now noticeably longer than the Li-O_{Ar} distance of 1.836(5) Å. Both the Li-N and Li-O_{diox} distances of 2.125(5) Å and 1.965(5) Å are similar to those seen in the previous complexes.

The hydrogen atom on the oxygen of the dimethylethanolamine forms a hydrogen bond with the oxygen of a neighboring aryloxy group. Single crystal X-ray diffraction using copper radiation was able to reliably show the hydrogen belonged to the dimethylethanolamine (O3-H1 = 0.94(4) Å) rather than the neighboring oxygen of the aryloxy group (O1-H1 = 1.62 Å). The pK_a of the two complexes are quite similar. The experimentally calculated pK_a of 2,4,6-trimethylphenol in water is 10.86 whereas the pK_a of dimethylethanolamine is 10.3.³¹ The solvent reaction mixture (hexane/dioxane) may play a key role in slightly changing the relative acidity of the two compounds, resulting in the formation of **2.6**.

Overall, the metal centers can be considered trigonal nodes, extending through two hydrogen-bonded units and one dioxane. This gives an extended two-dimensional structure with 6³-net topology (Figure 2.15).

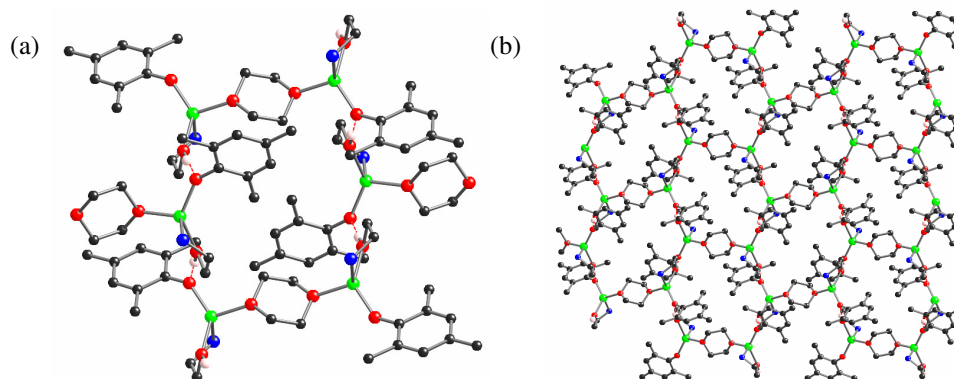
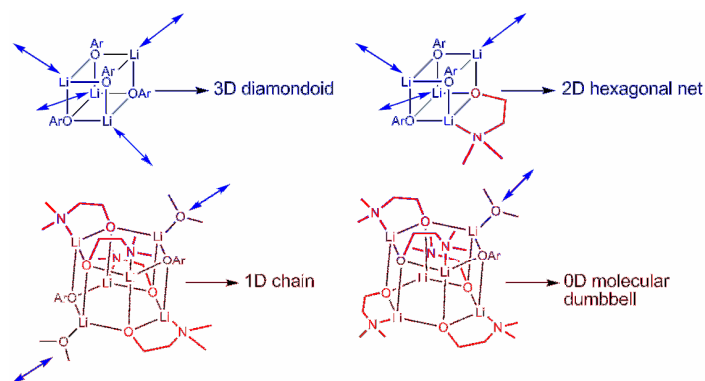


Figure 2.14 The extended structure of **2.6** highlighting (a) the hexagonal ring formed by a combination of hydrogen bonds and bridging dioxane, and (b) the two-dimensional 6^3 -net.

2.3 Summary

This study has demonstrated for the first time that lithiated mixed-anion aggregates can be used to rationally control extended supramolecular structure. In particular, the systematic incorporation of chelating ligands within such aggregates can block potential coordination sites for polymer growth. In turn, related lower dimensionality polymers may be prepared. In this case 3D diamondoid, 2D hexagonal net, 1D linear and 0D dumbbell structures have been identified (Scheme 3).



Scheme 2.3 Molecular SBUs in **2.1**, **2.2**, **2.4** and **2.5** illustrating their use as tetrahedral, trigonal, linear and single-bridging nodes.

With the exception of **2.3**, all of the materials form the highest dimensionality polymer possible from the tetrahedral, trigonal, linear and single-bridging SBUs. It is noteworthy that no terminally solvating dioxane adducts are prepared despite their assembly in the presence of a vast excess of the donor solvent. This suggests that entropy is a critical factor in determining the solid-state structures. In particular, bridging will result in expulsion of free dioxane into solution, which will be energetically favorable. This analysis is consistent with our previous studies of alkali metal coordination polymers, *i.e.* in general, the highest dimensionality network is produced if space filling requirements can be met.^{13,27} Complex **2.3** is an exception since there is insufficient local space available for solvation of all three lithium centers within the hexametallic aggregate.

An unanticipated consequence of altering the ratio of aryloxide and alkoxide anions was changing the basic aggregation state of the SBU. In the present case, a 3ArO:1ROLi aggregate could be prepared but increasing the ratio to equimolar quantities of the two anions resulted in formation of a hexametallic 3ArOLi:3ROLi aggregate. In hindsight this is not surprising, since ROLi is octameric in the solid state. Thus, increasing the stoichiometry of ROLi units in the mixed-anion complexes will change the relative stability of the various possible aggregated forms. In **2.3-2.5** this results in the preferential stabilization of hexametallic aggregates. Also, the set of complexes **2.1-2.5** and **2.7** is interesting from a molecular coordination chemistry perspective. To our knowledge, this series is unique in its stoichiometric diversity, forming 4:0, 3:1, 3:3, 2:4, 1:5, and 0:8 complexes.

Overall, the assembly of related, geometrically-constrained, mixed-anion complexes is likely to prove useful for a wide assortment of SBUs for future tailored-network assembly.

2.4 Experimental Section

2.4.1 General Procedures

All experimental manipulations were performed under a dry nitrogen atmosphere using standard Schlenk techniques, or in an argon-filled glovebox.³² All glassware was flame-dried under vacuum before use. Hexane was dried immediately before use by passage through columns of copper-based catalyst and alumina (Innovative Technology), and stored over 4 Å molecular sieves. Dioxane was purchased from Acros and was distilled over sodium benzophenone under N₂ prior to use. The phenol was purchased from Aldrich and was dried by recrystallization from hexane prior to use. BuLi (1.6 M solution in hexane) was purchased from Aldrich and standardized prior to use.³³ Deuterated solvents were purchased from Cambridge Isotope Laboratories and were dried by storage over 4 Å molecular sieves. ¹H and ¹³C NMR spectra were recorded on either a Varian Unity Plus 300 MHz or a Bruker AVANCE DPX-400 spectrometer at 293 K, and were referenced internally to the residual signals of the deuterated solvents.

2.4.2 X-ray Crystallography

Crystals were examined under Infineum V8512 oil. The datum crystal was affixed to a thin glass fiber mounted atop a tapered copper mounting-pin and transferred to the

100 K nitrogen stream of a Bruker APEX II diffractometer equipped with an Oxford Cryosystems 700 series low-temperature apparatus. Cell parameters were determined using reflections harvested from three sets of 12 $0.5^\circ \phi$ scans. The orientation matrix derived from this was passed to COSMO to determine the optimum data collection strategy.³⁴ Cell parameters were refined using reflections with $I \geq 10\sigma(I)$ harvested from the entire data collection. All data were corrected for Lorentz and polarization effects, as well as for absorption. Table A.1 and A.2 in the Appendix list the key crystallographic parameters for **2.1-2.6**. The structures were solved and refined using SHELXTL.³⁵ Structure solution was by direct methods. Non-hydrogen atoms not present in the direct methods solution were located by successive cycles of full-matrix least-squares refinement on F^2 . All non-hydrogen atoms were refined with parameters for anisotropic thermal motion. Hydrogen atoms were placed at idealized geometries and allowed to ride on the position of the parent atom. Hydrogen thermal parameters were set to 1.2× the equivalent isotropic U of the parent atom, 1.5× for methyl hydrogens.

2.4.3 Preparation and Characterization

2.1 $[(\text{ArOLi})_4 \cdot (\text{diox})_2] \supset 3(\text{diox})]_\infty$ - BuLi (2 mmol, 1.6 M solution in hexane) was added dropwise to a solution of 2,4,6-trimethylphenol (2 mmol, 272 mg) in dioxane (5 mL) to give a clear colorless solution. Storage of this solution under ambient conditions for 2 days resulted in the formation of clear colorless crystals. The product loses some dioxane on isolation, a typical ^1H NMR shows 0.38 equivalents of dioxane relative to the phenoxide, not 1.25 equivalents as in the crystal structure. Yield: 310 mg, 35.5%. δ_{H} (d_6 -DMSO, 293K) 2.02 (s, 6H, *o*-Me), 2.04 (s, 3H, *p*-Me), 3.58 (s, 6H, CH₂,

dioxane), 6.46 (s, 2H, *m*-H, Ph). δ_C (d_6 -DMSO, 293K) 18.46 (*o*-Me), 20.51 (*p*-Me), 66.42 (CH₂, dioxane), 115.35 (*p*-C, Ph), 123.98 (*o*-C, Ph), 127.80 (*m*-C, Ph), 164.54 (*i*-C, Ph).

2.2 $[\{(\text{ROLi})(\text{ArOLi})_3 \cdot (\text{diox})_{1.5}\} \supset 1/2(\text{C}_6\text{H}_{14})]_\infty$ - BuLi (4 mmol, 1.6 M solution in hexane) was added dropwise to a solution of 2,4,6-trimethylphenol (3 mmol, 408 mg) and dimethylethanolamine (1 mmol, 0.1 mL) in dioxane (2 mL) and hexane (16 mL) to give a light pink solution. A white precipitate formed, which completely dissolved on heating the solution to reflux. X-ray quality crystals were obtained by slowly cooling the resulting solution in a hot water bath. Crystalline yield: 220 mg, 33.7 %. δ_H (d_6 -benzene, 293K): 0.87-0.90 (broad, 3H, CH₃, hexane), 1.12-1.40 (broad, 4H, CH₂, hexane), 1.86 (s, 6H, NCH₃), 2.21 (s, 2H, NCH₂), 2.30 (s, 18H, *o*-Me), 2.31 (s, 9H, *p*-Me), 3.25 (s, 12H, dioxane), 3.89 (s, 2H, OCH₂), 6.90 (s, 6H, *m*-H, Ph). δ_C (d_6 -benzene, 293K): 18.82 (*o*-Me), 21.13 (*p*-Me), 45.04 (NCH₃), 60.86 (NCH₂), 65.82 (OCH₂), 67.31 (CH₂, dioxane), 123.47 (*p*-C, Ph), 124.73 (*o*-C, Ph), 130.12 (*m*-C, Ph), 161.07 (*i*-C, Ph).

2.3 $[\{(\text{ROLi})_3(\text{ArOLi})_3 \cdot (\text{diox})_{0.5}\}(\text{C}_6\text{H}_{14})]_\infty$ - BuLi (6 mmol, 1.6 M solution in hexane) was added dropwise to a solution of 2,4,6-trimethylphenol (3 mmol, 408 mg), dimethylethanolamine (3 mmol, 0.3 mL), and dioxane (5 mmol, 0.43 mL) in hexane (3 mL) to give a light pink solution. The solvent was removed in vacuo to give a light pink oil. The oil was taken up in hexane (5 mL). A white precipitate formed, which completely dissolved on heating the solution to reflux. X-ray quality crystals were obtained by slowly cooling the resulting solution in a hot water bath. Crystalline yield: 940 mg, 27.2 %. δ_H (d_6 -benzene, 293K): 0.87-0.90 (broad, 3H, CH₃, hexane), 1.15-1.40 (broad, 4H, CH₂, hexane), 1.84 (s, 18H, NCH₃), 2.19 (s, 6H, NCH₂), 2.27 (s, 18H, *o*-Me), 2.31 (s, 9H, *p*-Me), 3.12 (s, 4H, dioxane), 3.87 (s, 6H, OCH₂), 6.89 (s, 6H, *m*-H, Ph). δ_C (d_6 -benzene,

293K): 18.97 (*o*-Me), 21.39 (*p*-Me), 45.18 (NCH₃), 61.48 (NCH₂), 65.96 (OCH₂), 67.35 (CH₂, dioxane), 123.56 (*p*-C, Ph), 124.75 (*o*-C, Ph), 130.44 (*m*-C, Ph), 161.94 (*i*-C, Ph).

2.4 [(ROLi)₄(ArOLi)₂·(diox)]_∞ - BuLi (5 mmol, 1.6 M solution in hexane) was added dropwise to a solution of 2,4,6-trimethylphenol (1.25 mmol, 0.17 g) and dimethylethanolamine (3.75 mmol, 0.38 mL) in dioxane (3 mL) to give a light pink solution. The dioxane was removed in vacuo to give a light pink oil. The oil was taken up in hexane (4 mL). A white precipitate formed, which completely dissolved on heating the solution to reflux. X-ray quality crystals were obtained by cooling the solution to -20 °C for 48 h. Crystalline yield: 645 mg, 68.6 %. δ_H (*d*₆-benzene, 293K): 1.99 (s, 24H, NCH₃), 2.25 (s, 8H, NCH₂), 2.38 (s, 12H, *o*-Me), 2.43 (s, 6H, *p*-Me), 3.34 (s, 8H, dioxane), 3.89 (s, 24H, OCH₂), 7.00 (s, 4H, *m*-H, Ph). δ_C (*d*₆-benzene, 293K): 19.00 (*o*-Me), 21.37 (*p*-Me), 45.25 (NCH₃), 60.97 (NCH₂), 66.10 (OCH₂), 67.46 (CH₂, dioxane), 121.28 (*p*-C, Ph), 124.84 (*o*-C, Ph), 129.76 (*m*-C, Ph), 163.12 (*i*-C, Ph).

2.5 [(ROLi)₅(ArOLi)·(diox)_{0.5}]_∞ - BuLi (6 mmol, 1.6 M solution in hexane) was added dropwise to a solution of 2,4,6-trimethylphenol (1 mmol, 136 mg), dimethylethanolamine (5 mmol, 0.5 mL), and dioxane (5 mmol, 0.43 mL) in hexane (3 mL) to give a light yellow solution. The solvent was removed in vacuo to give a light yellow oil. The oil was taken up in hexane (3 mL). A white precipitate formed, which completely dissolved on heating the solution to reflux. X-ray quality crystals were obtained by slowly cooling the resulting solution in a hot water bath. Crystalline yield: 420 mg, 63.5 %. δ_H (*d*₆-benzene, 293K): 2.05 (s, 30H, NCH₃), 2.21 (s, 10H, NCH₂), 2.43 (s, 6H, *o*-Me), 2.56 (s, 3H, *p*-Me), 3.25 (s, 4H, dioxane), 3.80 (s, 10H, OCH₂), 7.05 (s, 2H, *m*-H, Ph). δ_C (*d*₆-benzene, 293K): 19.04 (*o*-Me), 21.38 (*p*-Me), 45.29 (NCH₃), 60.99

(NCH₂), 66.15 (OCH₂), 67.46 (CH₂, dioxane), 124.42 (*p*-C, Ph), 124.44 (*o*-C, Ph), 129.50 (*m*-C, Ph), 161.58 (*i*-C, Ph).

2.6 [(ArOLi)·(ROH)·(diox)_{0.5}]_∞ - BuLi (4 mmol, 1.6 M solution in hexane) was added dropwise to a solution of 2,4,6-trimethylphenol (2.5 mmol, 341 mg), dimethylethanolamine (2.5 mmol, 0.25 mL), and dioxane (5 mmol, 0.43 mL) in hexane (3 mL) to give a light pink solution. The solvent was removed in vacuo to give a light pink oil. The oil was taken up in hexane (4 mL). A white precipitate formed, which completely dissolved on heating the solution to reflux. X-ray quality crystals were obtained by slowly cooling the resulting solution in a hot water bath. Crystalline yield: 420 mg, 63.5 %. δ_{H} (*d*₆-benzene, 293K): 1.80 (s, 6H, NCH₃), 2.04 (s, 2H, NCH₂), 2.19 (s, 6H, *o*-Me), 2.19 (s, 3H, *p*-Me), 3.28 (s, 4H, dioxane), 3.60 (s, 2H, OCH₂), 6.75 (s, 2H, *m*-H, Ph). δ_{C} (*d*₆-benzene, 293K): 17.67 (*o*-Me), 20.97 (*p*-Me), 44.77 (NCH₃), 59.07 (NCH₂), 63.06 (OCH₂), 67.11 (CH₂, dioxane), 124.18 (*p*-C, Ph), 125.01 (*o*-C, Ph), 129.48 (*m*-C, Ph), 160.78 (*i*-C, Ph).

2.5 References

- [1] (a) Sanders, J. K. M. *Chem, Eur. J.* **1998**, *4*, 1378. (b) Zhao, H.; Heintz, R. A.; Ouyang, X.; Dunbar, K. R.; Campana C. F.; Rogers, R. D. *Chem. Mater.* **1999**, *11*, 736. (c) A. J. Fletcher, E. J. Cussen, T. J. Prior, M. J. Rosseinsky, C. J. Kepert and K. M. Thomas, *J. Am. Chem. Soc.* **2001**, *123*, 10001. (d) N. L. Rosi, J. Eckert, M. Eddaoudi, D. T. Vodak, J. Kim, M. O'Keefe and O. M. Yaghi, *Science* **2003**, *300*, 1127. (e) T. K. Maji, K. Uemura, H. -C. Chang, R. Matsuda and S. Kitagawa, *Angew. Chem., Int. Ed.* **2004**, *43*, 3331. (f) Chae, H. K.; Siberio-Perez, D. Y.; Kim, J.; Go, Y.; Eddaoudi, M.; Matzger, A. J.; O'Keefe, M.; Yaghi, O. M. *Nature* **2004**, *427*, 523. (g) Mueller, U.; Schubert, M.; Teich, F.; Puetter, H.; Schierle-Arndt, K.; Pastré, J. *J. Mater. Chem.* **2006**, *16*, 626.

- [2] Haiduc, I.; Edelman, F. T. *Supramolecular Organometallic Chemistry*, Wiley-VCH, New York, 1999.
- [3] (a) Braga, D.; Grepioni, F. *Coord. Chem. Rev.* **1999**, *183*, 19. (b) Desiraju, G. R. *Dalton Trans.* **2000**, 3745. (c) Johansson, R.; Öhrström, L.; Wendt, O. F. *Cryst. Growth Des.* **2007**, *7*, 1974.
- [4] Moulton, B.; Zaworotko, M. J. *Chem. Rev.* **2001**, *101*, 1629.
- [5] (a) Russell, V. A.; Evans, C. C.; Li, W.; Ward, M. D. *Science* **1997**, *276*, 575. (b) Eddaoudi, M.; Kim, J.; Rosi, N.; Vodak, D.; Wachter, J.; O'Keeffe, M.; Yaghi, O. M. *Science* **2002**, *295*, 469. (c) Maji, T. K.; Ohba, M.; Kitagawa, S. *Inorg. Chem.* **2005**, *44*, 9225. (d) Li, J. -R.; Bu, X. -H.; Jiao, J.; Du, W. -P.; Xu, X. -H.; Zhang, R. -H. *Dalton Trans.* **2005**, 464. (e) Halper, S. R.; Do, L.; Stork, J. R.; Cohen, S. M. *J. Am. Chem. Soc.* **2006**, *128*, 15255. (f) Biradha, K.; Sarkar, M.; Rajput, L. *Chem. Commun.* **2006**, 4169. (g) Yang, E. -C.; Zhao, H. -K.; Ding, B.; Wang, X. -G.; Zhao, X. -J. *Cryst. Growth Des.* **2007**, *7*, 2009. (h) Du, M.; Jiang, X. -J.; Zhao, X. -J. *Inorg. Chem.* **2007**, *46*, 3984. (i) Chen, B.; Ma, S.; Zapata, F.; Fronczek, F. R.; Lobkovsky, E. B.; Zhou, H. -C. *Inorg. Chem.* **2007**, *46*, 1233.
- [6] (a) Abrahams, B. F.; Hawley, A.; Haywood, M. G.; Hudson, T. A.; Robson, R.; Slizys, D. A. *J. Am. Chem. Soc.* **2004**, *126*, 2894. (b) Li, Z.; Li, M.; Zhou, X. -P.; Wu, T.; Li, D.; Ng, S. W. *Cryst. Growth Des.* **2007**, *7*, 1992. (c) Forster, P. M.; Guillou, N.; Tafuya, M. M.; Cheetham, A. K.; Férey, G. *Angew. Chem. Int. Ed.* **2007**, *46*, 5877. (d) Du, M.; Zhang, Z. -H.; Tang, L. -F.; Wang, X. -G.; Zhao, X. -J.; Batten, S. R. *Chem. Eur. J.* **2007**, *13*, 2578. (e) Hitzbleck, J.; Deacon, G. B.; Ruhlandt-Senge, K. *Eur. J. Inorg. Chem.* **2007**, 592.
- [7] (a) Swift, J. A.; Pivovar, A. M.; Reynolds, A. M.; Ward, M. D. *J. Am. Chem. Soc.* **1998**, *120*, 5887. (b) Withersby, M. A.; Blake, A. J.; Champness, N. R.; Cooke, P. A.; Hubberstey, P.; Li, W. -S.; Schröder, M. *Inorg. Chem.* **1999**, *38*, 2259. (c) Blake, A. J.; Brooks, N. R.; Champness, N. R.; Crew, M.; Deveson, A.; Fenske, D.; Gregory, D. H.; Hanton, L. R.; Hubberstey, P.; Schröder, M. *Chem. Commun.* **2001**, 1432. (d) Kobayashi, K.; Sato, A.; Sakamoto, S.; Yamaguchi, K. *J. Am. Chem. Soc.* **2003**, *125*, 3035. (e) Oh, M.; Carpenter, G. B.; Sweigart, D. A. *Organometallics* **2003**, *22*, 2364. (f) Lee, I. S.; Shin, D. M.; Chung, Y. K. *Chem. Eur. J.* **2004**, *10*, 3158. (g) Choi, H. J.; Suh, M. P. *J. Am. Chem. Soc.* **2004**, *126*, 15844. (h) Long, D. -L.; Hill, R. J.; Blake, A. J.; Champness, N. R.; Hubberstey, P.; Wilson, C.; Schröder, M. *Chem. Eur. J.* **2005**, *11*, 1348. (i) Maji, T. K.; Mostafa, G.; Matsuda, R.; Kitagawa, S. *J. Am. Chem. Soc.* **2005**, *127*, 17152. (j) Du, M.; Zhao, X. -J.; Guo, J. -H.; Batton, S. R. *Chem. Commun.* **2005**, 4836. (k) Wang, X. -Y.; Wang, L.; Wang, Z. -M.; Gao, S. *J. Am. Chem. Soc.* **2006**, *128*, 674.

- [8] Surblé, S.; Millange, F.; Serre, C.; Férey, G.; Walton, R. I. *Chem. Commun.* **2006**, 1518.
- [9] (a) Masaoka, S.; Tanaka, D.; Nakanishi, Y.; Kitagawa, S. *Angew. Chem. Int. Ed.* **2004**, *43*, 2530. (b) Sun, D.; Ke, Y.; Mattox, T. M.; Ooro, B. A.; Zhou, H. –C. *Chem. Commun.* **2005**, 5445. (c) Dan, M.; Rao, C. N. R. *Angew. Chem., Int. Ed.* **2006**, *45*, 281.
- [10] Go, Y. B.; Wang, X.; Anokhina, E. V.; Jacobson, A. J. *Inorg. Chem.* **2005**, *44*, 8265.
- [11] Ockwig, N. W.; Delgado-Friedrichs, O.; O’Keeffe, M.; Yaghi, O. M. *Acc. Chem. Res.* **2005**, *38*, 176.
- [12] (a) Dan, M.; Rao, C. N. R. *Angew. Chem. Int. Ed.* **2006**, *45*, 281. (b) Cheetham, A. K.; Rao, C. N. R.; Feller, R. K. *Chem. Commun.* **2006**, 4780.
- [13] (a) MacDougall, D. J.; Morris, J. J.; Noll, B. C.; Henderson, K. W. *Chem. Commun.* **2005**, 456. (b) MacDougall, D. J.; Noll, B. C.; Henderson, K. W. *Inorg. Chem.* **2005**, *44*, 1181. (c) Morris, J. J.; Noll, B. C.; Henderson, K. W. *Cryst. Growth Des.* **2006**, *6*, 1071. (d) Morris, J. J.; Noll, B. C.; Honeyman, G. G.; Kennedy, A. R.; Mulvey, R. E.; Henderson, K. W. *Chem. –Eur. J.* **2007**, *13*, 4418. (e) Morris, J. J.; Noll, B. C.; Henderson, K. W. *Chem. Commun.* **2007**, 5191. (f) Morris, J. J.; Noll, B. C.; Schultz, A. J.; Piccoli, P. M. B.; Henderson, K. W. *Inorg. Chem.* **2007**, *46*, 10473.
- [14] For related work on alkaline earth metals see: (a) Rood, J. A.; Noll, B. C.; Henderson, K. W. *Inorg. Chem.* **2006**, *45*, 5521. (b) Rood, J. A.; Noll, B. C.; Henderson, K. W. *Main Group Chem.* **2006**, *5*, 21. (c) Rood, J. A.; Boggess, W. C.; Noll, B. C.; Henderson, K. W. *J. Am. Chem. Soc.* **2007**, *129*, 13675.
- [15] For earlier studies on internally solvating ligands see: (a) Henderson, K. W.; Kennedy, A. R.; McKeown, A. E.; Strachan, D. S. *J. Chem. Soc., Dalton Trans.* **2000**, 4348. (b) Henderson, K. W.; Kennedy, A. R.; Macdonald, L.; MacDougall, D. J. *Inorg. Chem.* **2003**, *42*, 2839. (c) Henderson, K. W.; Kennedy, A. R.; MacDougall, D. J.; Shanks, D. *Organometallics* **2002**, *21*, 606.
- [16] For more information on lithiated mixed-anion systems see: (a) Pratt, L. M. *Mini-Rev. Org. Chem.* **2004**, *1*, 209. (b) Ko, B. –T.; Lin, C. –C. *J. Am. Chem. Soc.* **2001**, *123*, 7973. (c) Xu, F.; Reamer, R. A.; Tillyer, R.; Cummins, J. M.; Grabowski, E. J. J.; Reider, P. J.; Collum, D. B.; Huffman, J. C. *J. Am. Chem. Soc.* **2000**, *122*, 11212. (d) Ko, B. –T.; Lin, C. –C. *J. Am. Chem. Soc.* **2001**, *123*, 7973. (e) Huang, B. –H.; Ko, B. –T.; Athar, T.; Lin, C. –C. *Inorg. Chem.* **2006**, *45*, 7348.
- [17] Andrews, P. C.; MacLellan, J. G.; Mulvey, R. E.; Nichols, P. J. *J. Chem. Soc., Dalton Trans.* **2002**, 1651.

- [18] Henderson, K. W.; Noll, B. C.; Kennedy, A. R.; MacDougall, D. J. *Dalton Trans.* **2006**, 1875.
- [19] (a) Jackman, L. M.; DeBrosse, C. W. *J. Am. Chem. Soc.* **1983**, *105*, 4177. (b) Jackman, L. M.; Scarmoutzos, L. M.; DeBrosse, C. W. *J. Am. Chem. Soc.* **1987**, *109*, 5355. (c) Jackman, L. M.; Smith, B. D. *J. Am. Chem. Soc.* **1988**, *110*, 3829. (d) Jackman, L. M.; Rackiewicz, E. F. *J. Am. Chem. Soc.* **1991**, *113*, 1202. (e) Jackman, L. M.; Rackiewicz, E. F.; Bensei, A. J. *J. Am. Chem. Soc.* **1991**, *113*, 4101. (f) Jackman, L. M.; Petrei, M. M.; Smith, B. D. *J. Am. Chem. Soc.* **1991**, *113*, 3451. (g) Jackman, L. M.; Chen, X. *J. Am. Chem. Soc.* **1992**, *114*, 403. (h) Jackman, L. M.; Çizmeciyen, D.; Williard, P. G.; Nichols, M. A. *J. Am. Chem. Soc.* **1993**, *115*, 6262. (i) Jackman, L. M.; Çizmeciyen, D. *Magn. Reson. Chem.* **1996**, *34*, 14.
- [20] (a) Arnett, E. M.; Nichols, M. A.; McPhail, A. T. *J. Am. Chem. Soc.* **1990**, *112*, 7059. (b) Reich, H. J.; Goldenberg, W. S.; Sanders, A. W.; Jantzi, K. L.; Tzschucke, C. C. *J. Am. Chem. Soc.* **1999**, *118*, 2981.
- [21] (a) Aubrecht, K. B.; Lucht, B. L.; Collum, D. B. *Organometallics* **1999**, *18*, 2981. (b) McNeil, A. J.; Toombes, G. E. S.; Gruner, S. M.; Lobkovsky, E.; Collum, D. B.; Chandramouli, S. V.; Vanasse, B. J.; Ayers, T. A. *J. Am. Chem. Soc.* **2004**, *126*, 16559.
- [22] The Cambridge Structural Database, version 5.28, updates August 2007. Allen, F. H. *Acta Crystallogr., Sect. B* **2002**, *58*, 380.
- [23] (a) Ko, B. -T.; Lin, C. -C. *J. Am. Chem. Soc.* **2001**, *123*, 7973. (b) Huang, B. -H.; Ko, B. -T.; Athar, T.; Lin, C. -C. *Inorg. Chem.* **2006**, *45*, 7348.
- [24] The dimensions of the channels are measured by the closest transannular H-H distances.
- [25] The PLATON software package was used to calculate the void space: Spek, A. L. *Acta Crystallogr., Sect. A* **1990**, *46*, 1016.
- [26] Delgado-Friedrichs, O.; O'Keeffe, M.; Yaghi, O. M. *Phys. Chem. Chem. Phys.* **2007**, *9*, 1035.
- [27] For a discussion of efficient space filling see: Mecozzi S.; Rebek Jr., J. *Chem. Eur. J.* **1998**, *4*, 1016.
- [28] Iravani, E.; Neumuller, B. Z. *Anorg. Allg. Chem.* **2006**, *632*, 289.

- [29] (a) Harder, S.; Boersma, J.; Brandsma, L. *J. Organomet. Chem.* **1988**, 339, 7. (b) McGeary, M. J.; Folting, K.; Streib, W. E.; Huffman, J. C.; Caulton, K. G. *Polyhedron*, **1991**, 10, 2699. (c) Angelis, S. D.; Solari, E.; Gallo, E.; Floriani, C.; Chiesi-Villa, A.; Rizzoli, C. *Inorg. Chem.* **1992**, 31, 2520. (d) Neander, S.; Tio, F. E.; Buschmann, R.; Behrens, U.; Olbrich, F. *J. Organomet. Chem.* **1999**, 582, 58. (e) Neader, S.; Behrens, U.; Olbrich, F. *J. Organomet. Chem.* **2000**, 604, 59.
- [30] (a) Müller, B.; Krausse, J. *J. Organomet. Chem.* **1972**, 44, 141. (b) Cramer, R. E.; Bruck, M. A.; Gilje, J. W. *Organometallics*, **1986**, 5, 1496. (c) Evans, W. J.; Dominguez, R.; Levan, K. R.; Doedens, R. J. *Organometallics*, **1985**, 4, 1836. (d) Uhl, W.; Klinkhammer, K. –W.; Layh, M.; Massa, W. *Chem. Berichte* **1991**, 124, 279. (e) Bryan, J. C.; Sachleben, R. A.; Lavis, J. M.; Davis, M. C.; Burns, J. H.; Hay, B. P. *Inorg. Chem.* **1998**, 37, 2749. (f) Schiefer, M.; Reddy, N. D.; Ahn, H. –J.; Stasch, A.; Roesky, H. W.; Schlicker, A. C.; Schmidt, H. –G.; Noltemeyer, M.; Vidovic, D. *Inorg. Chem.* **2003**, 42, 4970. (g) Kerton, F. M.; Kozak, C. M.; Lüttgen, K.; Willans, C. E.; Webster, R. J.; Whitwood, A. C. *Inorg. Chim. Acta* **2006**, 359, 2819.
- [31] Jover, J.; Bosque, R.; Sales, J. *QSAR Comb. Sci.* **2007**, 26, 385.
- [32] Schriver, D. F.; Drezdon, M. A. *The Manipulation of Air-Sensitive Compounds*, Wiley, New York, 1986.
- [33] Love, B. E.; Jones, E. G. *J. Org. Chem.* **1999**, 64, 3755.
- [34] Kaercher, J. COSMO, Bruker-Nonius AXS, Inc., Madison, Wisconsin, USA, 2003.
- [35] Sheldrick, G. M. University of Göttingen, Göttingen (Germany), 2001.